*JKAU: Eng. Sci.*, **Vol. 1**, pp. 49-63 (1409 A.H./1989 A.D.)

# A Four-Legged Mobile Robot for Teaching and Demonstration

A.R. MANNAA, F. DEHLAWI* and M. AKYURT
*Mechanical Engineering Department and Electrical and Computer Engineering Department*, College of Engineering,
King Abdulaziz University, Jeddah, Saudi Arabia.*

ABSTRACT Design conditions are elaborated for a novel four-legged teaching/demonstration robot that can grip 500 g blocks of wood, load them on a platform on its back, transport them to a different location, and unload them there. To this end, various animation mechanisms are studied for their suitability for four-legged locomotion. One selected mechanism is used to characterize the level walking behaviour of the robot.

Adaptation of a three-link arm as well as the design of a suitable gripper to the mainframe are discussed.

## Introduction

Design studies are being carried out that will lead to the development of a novel four-legged teaching and demonstration robot which is capable of picking up wooden blocks of about 500 g, storing them on a platform on its back, transporting them to another destination, and depositing them there. To this end legged locomotion, arm motion, and walking behaviour are studied.

Legged locomotion can be accomplished in a variety of ways, the number of legs ranging from two to many. Each set of legs in turn exhibits various modes or gaits[1].

We discuss below various linkage configurations that permit four-legged locomotion of a mainframe. Mechanical design considerations are summarized next for a three-link robot arm that is to be assembled on the mainframe. Finally, the walking behaviour of the robot itself is studied. The electronics and test results are to be addressed in a separate communication.

## Mechanisms for Four-Legged Locomotion

A mechanism *R*-1 that consists of two crossed four-bar linkages, which are cranked by the same member $A_0A$[2] is shown in Fig. 1. Points $A_0$, $B_0$, and $D_0$ represent the mainframe, which is considered fixed for convenience. $D_0E$ and *BC* are two of the legs. In practice, one would use two sets of this mechanism for four-legged motion.

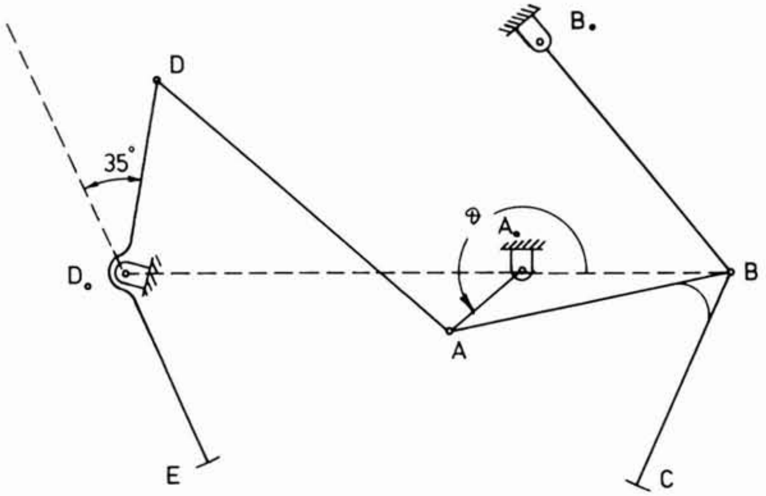

FIG. 1. Mechanism *R*-1.

It is clear, from Fig. 1, that the leg $D_0E$ describes a circular arc. To study the motion of the (front) leg *BC*, we may assume for comparison purposes, the dimensions and magnitudes listed in Table 1. The corresponding foot trajectory (point *C*) rela-

TABLE 1. Kinematics of Mechanism *R*-1.

| Crank angle 0° | ${}^{\omega}AC$ rad/s | ${}^{\alpha}AC$ rad/s$^2$ | ${}^{\omega}DD_0E$ rad/s | ${}^{\alpha}DD_0E$ rad/s$^2$ |
|---|---|---|---|---|
| 0 | –1 | –10 | 0 | 15 |
| 30 | –2 | – 4 | 1 | 12 |
| 60 | –1 | 6 | 1 | 5 |
| 90 | –1 | 15 | 1 | – 3 |
| 120 | –0 | 17 | 1 | –10 |
| 150 | 1 | 13 | 1 | –15 |
| 180 | 1 | 6 | –0 | –15 |
| 210 | 1 | – 1 | –1 | –11 |
| 240 | 1 | – 6 | –1 | – 5 |
| 270 | 1 | –10 | –1 | 3 |
| 300 | 0 | –12 | –1 | 10 |
| 330 | –0 | –13 | –1 | 14 |
| 360 | –1 | –10 | 0 | 15 |

$A_0A = 0.03$ m $AD = 1.00$ m $A_0B_0 = 0.36$ m $A_0D_0 = 1.05$ m
$AB = 0.30$ m $D_0D = 0.20$ m $AC = 0.30$ m $D_0E = 0.30$ m
$BC = 0.44$ m $B_0B = 0.51$ m $A_0D_0$ is perpendicular to $A_0B_0$ and angular velocity of $A_0A$ is uniform, and equal to 10 rad/s tawafwisē.

tive to the crankshaft is shown in Fig. 2, and angular motions of the feet in Table 1. The angles shown on the trajectory of Fig. 2 indicate crank displacements. The hind foot $DD_0E$ swings a total of 17° each way during one cycle. It is to be noted in Table 1 that the legs move in opposite directions, and that angular velocities and angular accelerations remain reasonably small throughout the cycle.

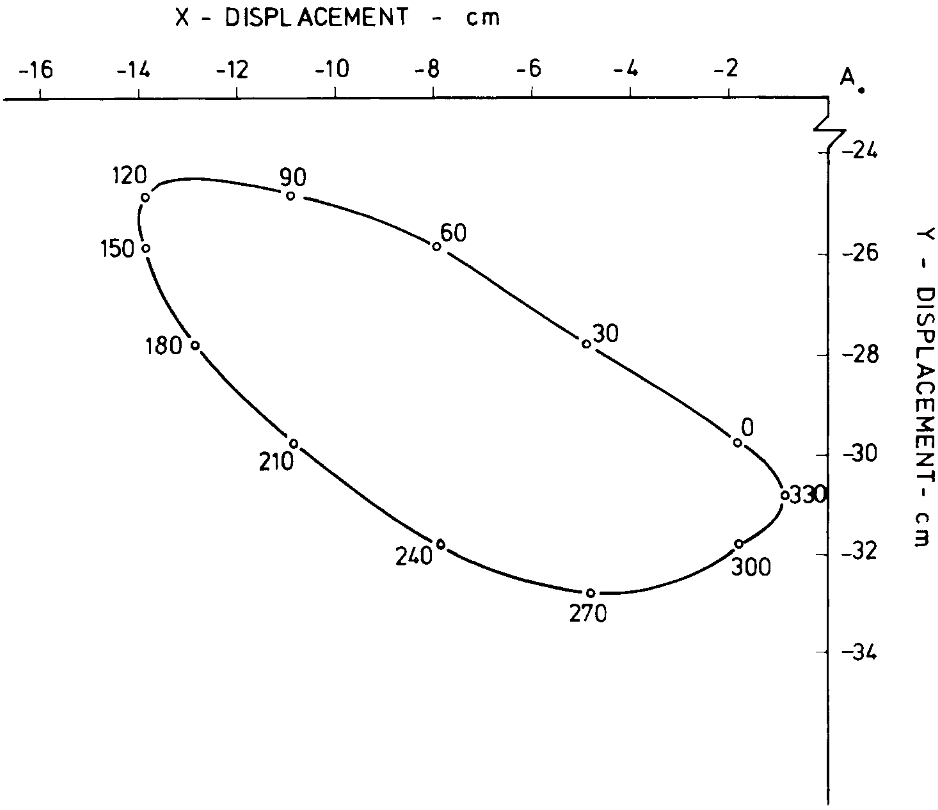

FIG. 2. Foot trajectory for *R*-1.

A second animation mechanism (*R*-2) is shown in Fig. 3, where the rear leg is actuated in the manner of *R*-1. The front leg, however, utilizes an inversion of the slider-crank mechanism. Assuming the dimensions listed in Table 2, it follows that the hind foot $BB_0E$ swings 16° either way during the cycle. The front foot describes an egg-like path in (Fig. 4). It is of interest to note that the feet move in opposite directions (Table 2). Moderate values of angular velocities and angular accelerations prevail.

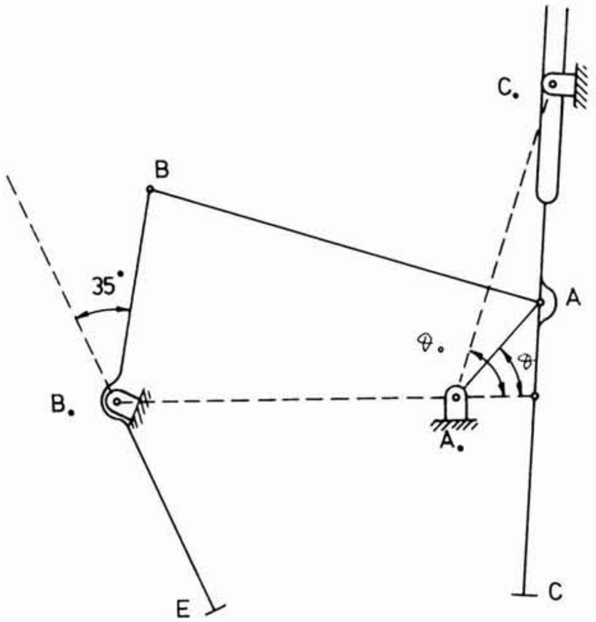

FIG. 3. Mechanism $R$-2.

TABLE 2. Kinematic Analysis of Mechanism $R$-2.

| Angle | $A_0 A C_0$ | | $A_0 A B B_0$ | |
|---|---|---|---|---|
| | $^{\omega}AC$ | $^{\alpha}AC$ | $^{\omega}B_0E$ | $^{\alpha}B_0E$ |
| 0 | 0.1 | –8.2 | 0.3 | 15.1 |
| 30 | –0.4 | –8.4 | 1.0 | 11.7 |
| 60 | –0.8 | –5.6 | 1.4 | 5.0 |
| 90 | –0.9 | 0.0 | 1.5 | –2.8 |
| 120 | –0.8 | 5.6 | 1.2 | –9.9 |
| 150 | –0.4 | 8.4 | 0.5 | –14.5 |
| 180 | 0.1 | 8.2 | –0.3 | –15.1 |
| 210 | 0.4 | 6.0 | –1.0 | –11.4 |
| 240 | 0.7 | 3.1 | –1.4 | –4.7 |
| 270 | 0.8 | 0.0 | –1.5 | 2.9 |
| 300 | 0.7 | –3.1 | –1.1 | 9.7 |
| 330 | 0.4 | –6.0 | –0.5 | 14.2 |
| 360 | 0.1 | –8.2 | 0.3 | 15.1 |

$A_0A = 0.03$ m $A_0C_0 = 0.36$ m $A_0B_0 = 1.05$ m $\Theta_0 = 90.1°$
$AB = 1.00$ m $AC = B_0E = 0.30$ m $B_0B = 0.20$ m, and
angular velocity of $A_0A$ is uniform, and equal to 10 rad/s tawafwise.

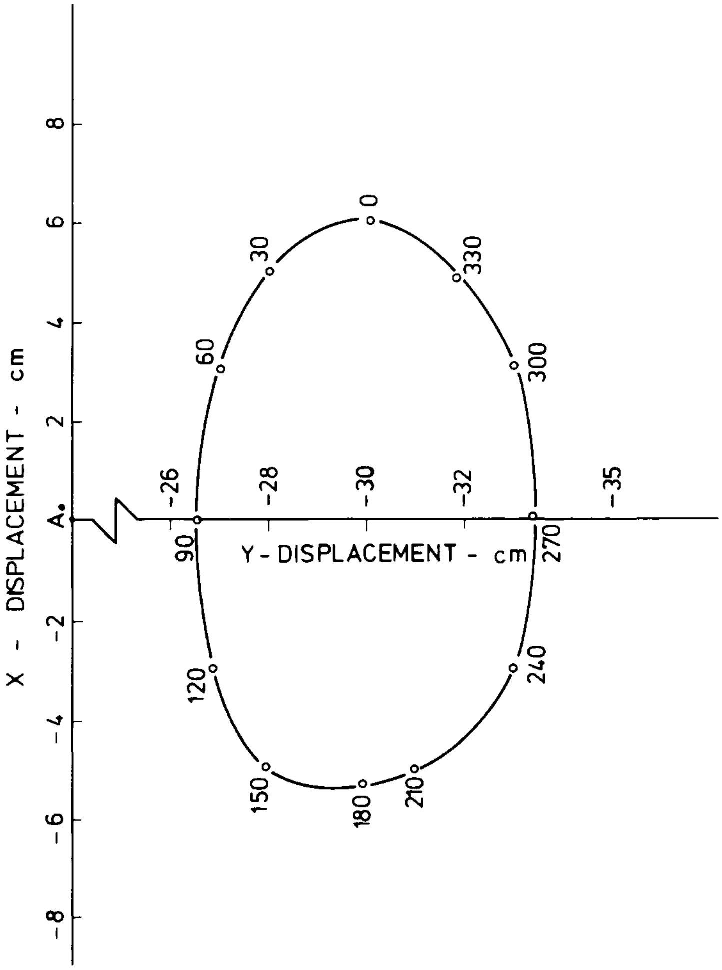

FIG. 4. Foot trajectory for *R*-2.

Perhaps the most common mechanism employed in animated toys is *R*-3[3,4], which is shown in Fig. 5. It differs from *R*-2 by the rigid extension *AD*. Letting[5]

$A_0A = 0.03\,\mathrm{m}$ $\quad A_0C_0 = 0.22$ $\quad A_0B_0 = 1.05$

$B_0B = 0.20$ $\quad AD = 0.07$ $\quad \Phi = 70°$

$BD = 0.93$ $\quad \Theta_0 = 110°$ $\quad B_0E = AC = 0.30$

angular velocity of $A_0A$ = 10 rad/s tawafwise (counter clockwise) and constant.

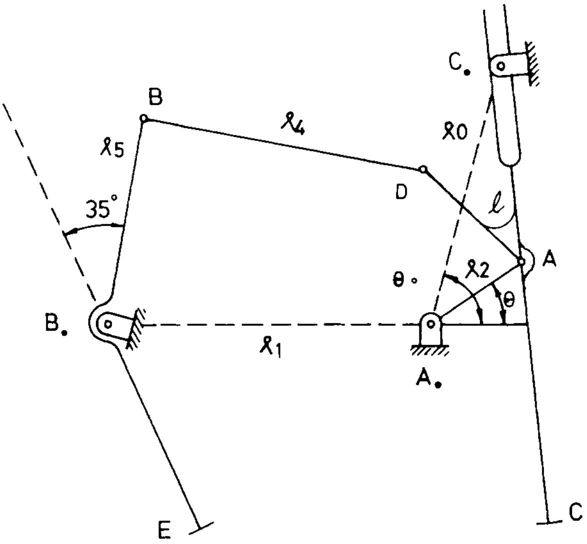

FIG. 5. Mechanism $R$-3.

One concludes again that the feet move in opposite directions, and that the motion is smooth. The trajectory of the front foot, however, is more like an ellipse (Fig. 6) than for $R$-2 (Fig. 4).

One other mechanism ($R$-4) that is occasionally encountered in animated toys is sketched in Fig. 7. $R$-4 is essentially two inversions of the slider-crank mechanism in tandem. Since $B_0$ and $C_0$ are fixed points, both feet describe circular arcs in the suspended state. Table 3 summarizes the kinematics for $R$-4. The front legs oscillate by 9°, and the rear legs by 8° each half cycle, and in opposite directions.

Comparing mechanisms $R$-1 to $R$-4, it is observed that $R$-1, $R$-2, and $R$-3 possess a certain degree of obstacle-crossing ability since the front foot is raised off the ground part of the time. $R$-4 does not exhibit such behaviour. The rear legs in all mechanisms are expected to skid during the non-tracing phase of their motions. A friction wheel equipped with a one-way clutch may, therefore, help reduce parasitic drag on the rear legs (*see:* Fig. 14). When walking, however, feet of a horse on a given side move in the same direction.

We choose for further study a mechanism of type $R$-3 to enable the robot to trot like a horse, and to be able to go over small obstacles. Dimensional information on this mainframe is summarized in Table 4[5].

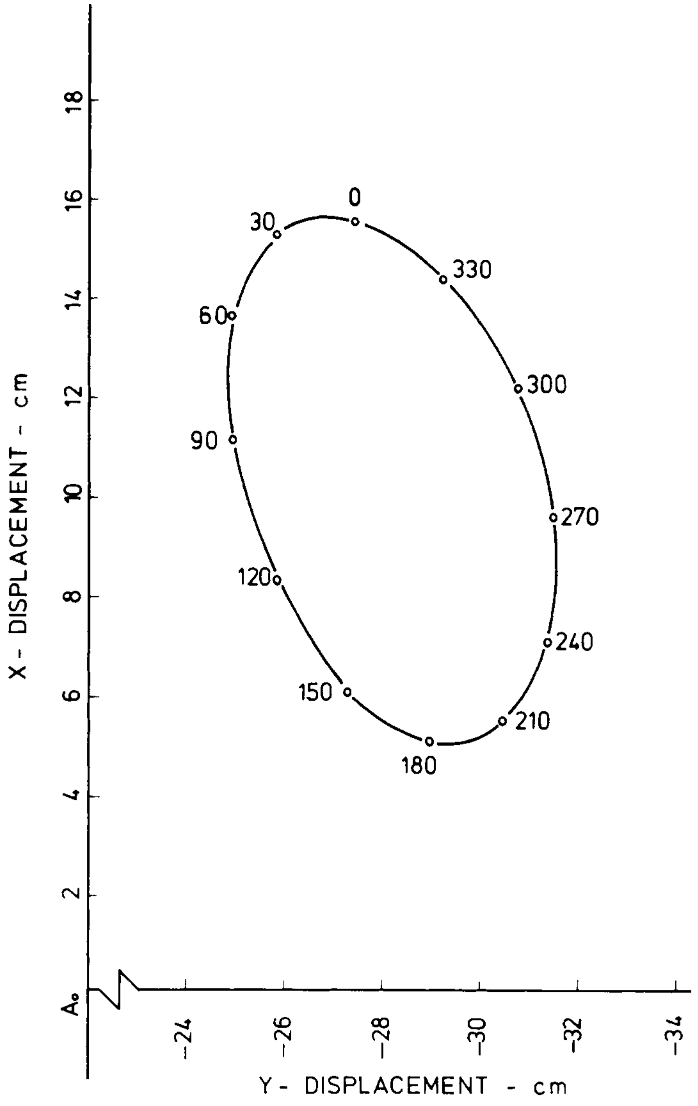

FIG. 6. Front foot trajectory for *R*-3.

## The Arm and Its Gripper

The design of the arm depends, to a considerable extent, on the physical dimensions as well as the configuration of the mainframe. This is because the arm is to be mounted on top of the mainframe. Figure 8 outlines the overall dimensions selected for the mainframe. The platform will feature a transparent deck so as to enable the viewing of the various electronic and mechanical components that will be installed on the mainframe. This is compatible with the objective of developing a robot for teaching and demonstration.

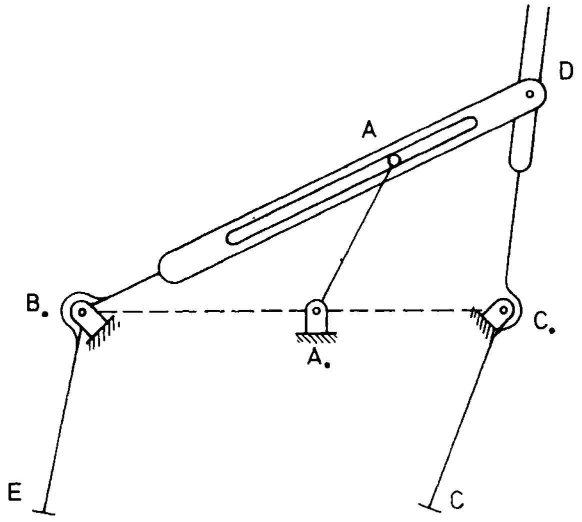

FIG. 7. Mechanism $R$-4

TABLE 3. Kinematics of Mechanism $R$-4.

| 0° | $^{\omega}B_0D$ rad/s | $^{\alpha}B_0D$ rad/s$^2$ | $^{\omega}CD$ rad/s | $^{\alpha}CD$ rad/s$^2$ |
|---|---|---|---|---|
| 0 | 0.6 | –0.0 | –0.7 | 0.0 |
| 30 | 0.6 | –2.6 | –0.6 | 3.0 |
| 60 | 0.4 | –5.1 | –0.4 | 5.6 |
| 90 | 0.0 | –6.6 | –0.0 | 7.2 |
| 120 | –0.3 | –6.3 | 0.3 | 6.3 |
| 150 | –0.6 | –3.8 | 0.7 | 4.3 |
| 180 | –0.7 | 0.3 | 0.8 | –0.3 |
| 210 | –0.6 | 4.2 | 0.7 | –4.7 |
| 240 | –0.3 | 6.4 | 0.3 | –7.0 |
| 270 | 0.0 | 6.6 | –0.0 | –7.2 |
| 300 | 0.4 | 5.2 | –0.4 | –5.8 |
| 330 | 0.6 | 2.9 | –0.6 | –3.3 |
| 360 | 0.6 | 0.2 | –0.7 | –0.2 |

$B_0A_0 = 0.45$ m $A_0C_0 = 0.60$ m $A_0A = 0.03$ m $B_0D = 0.55$ m and angular velocity of $A_0A$ is uniform, and equal to 10 rad/s tawafwise.

TABLE 4. Set of Dimensions for the Mainframe (See Fig. 5, 11 and 12).

$\phi = 80°$
$\psi = 35°$
$\theta_0 = 91°$
$\theta_G = 10°$

$l_0 = 28$ cm
$l_1 = 105$ cm
$l_2 = 3$ cm
$l_4 = 93$ cm
$l_5 = 18$ cm
$l_G = 35$ cm

$B_0E = 30$ cm
$WI = 60$ cm
$AC = 30$ cm

It was further decided that loading and unloading will be done from sides *a*, *b* and *d* of the mainframe (Fig. 8), and not from the electronics bay area (side *c*). Furthermore, a counterweight was envisaged to be placed on member *BC*, at a distance of 0.40 m from *B*, for the purpose of reducing the torque requirement at *B*. For reasons

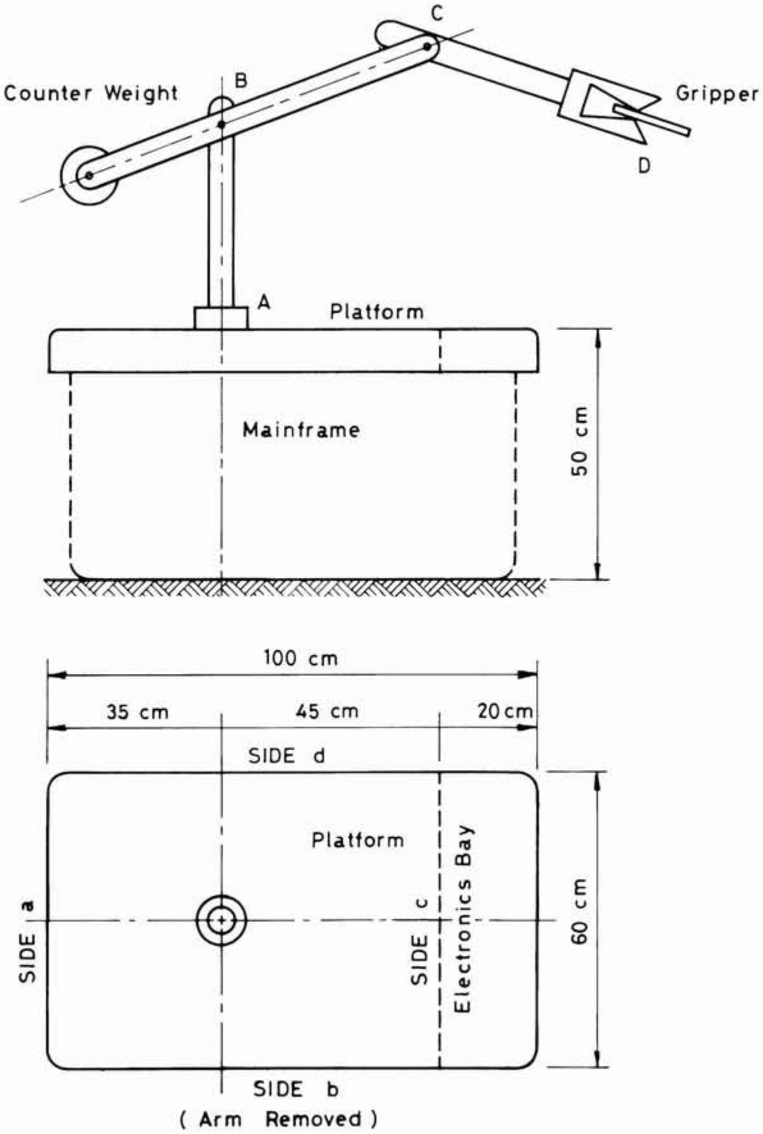

FIG. 8. Overall view of the robot.

of stability, the arm, which has three degrees of freedom, was required to be in its folded-up position (all members parallel) during locomotion. Considerations including these as well as work area, torque, stiffness, and stability requirements led to the selection of the following link lengths[6]:

$AB = 0.26$ m $\qquad BC = 0.66$ m $\qquad CD = 0.61$ m

which result in a total horizontal reach of 1.01 m at ground level.

A simple gripper with a linear input may be envisioned as in Fig. 9, where the half jaw opening, $y$, is

$$y = y_0 + (l_0 - l)\sin\Theta + l_1 \sin(\Theta - \Phi) \tag{1}$$

where $l = -x/\cos(\Theta + 180)$
$\Theta = tan\,(-y_0/-x) - 180°$

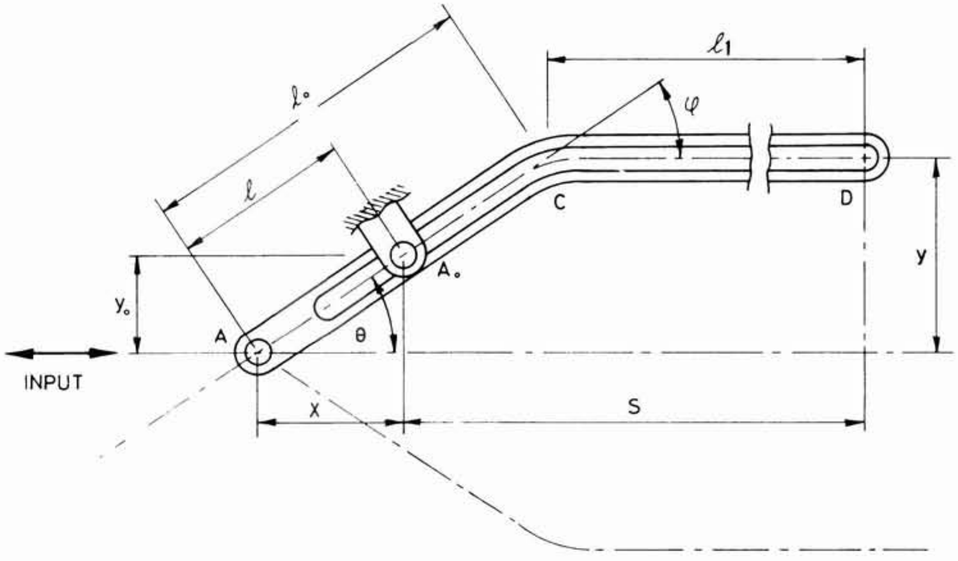

FIG. 9. The Gripper.

The grip depth $S$ then becomes

$$S = (l_0 - l)\cos\ \Theta + l_1 \cos(\Theta - \Phi) \tag{2}$$

It would be desirable to keep $x < 4$ cm, and $S$ relatively constant for a $y_{max}$ of 10 cm, corresponding to an aperture of 20 cm. Also the magnification factor: $y_0/S$ must be $>0.5$ if the input force in the direction of $x$ is to remain reasonably small. One set of dimensions that meets these constraints is

$$y_0 = 5\text{ cm} \qquad l_0 = 10\text{ cm} \qquad l_1 = 15\text{ cm} \qquad \text{and} \qquad \Phi = 90^\circ$$

Figure 10 shows the completed gripper as assembled on the arm.

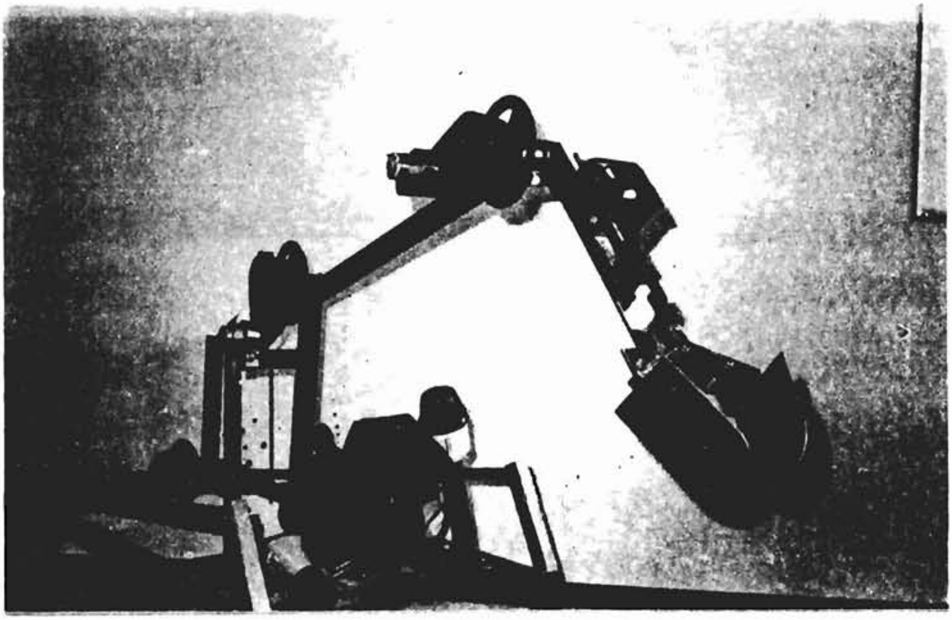

FIG. 10. The gripper and the arm.

## Walking on Four Legs

Figure 11 depicts the chosen mechanism $R$-3 in duplicate, as would be required on a four-legged platform. Point $G$ indicates the location of the center of mass of the entire suspended assembly, including the arm. The common crank $A_1A_0A$ causes the two pairs of feet $D_1$, $E_1$, and $D$, $E$ to move in opposite directions.

In actual walking, three of the feet are normally grounded, the two rear feet and one of the front feet. The grounded diagonal feet do the tracting. Considering the case when $D_1$, $E$, and $E_1$ are grounded, the plane passing through these points in the suspended robot (Fig. 12) needs to be rotated until its normal becomes normal to level ground. The associated rotation tensor for rectilinear walking becomes

$$A = \left| \begin{array}{ccc} \cos\Phi & \sin\Phi & 0 \\ -\cos\psi\sin\Phi & \cos\psi\cos\Phi & \sin\psi \\ \sin\psi\sin\Phi & -\sin\psi\cos\Phi & \cos\psi \end{array} \right| \tag{3}$$

where

$$\tan \Phi = [YD - YE] / XD - XE] \quad (4)$$

$$\tan \psi = [EY - YE] / WI \quad (5)$$

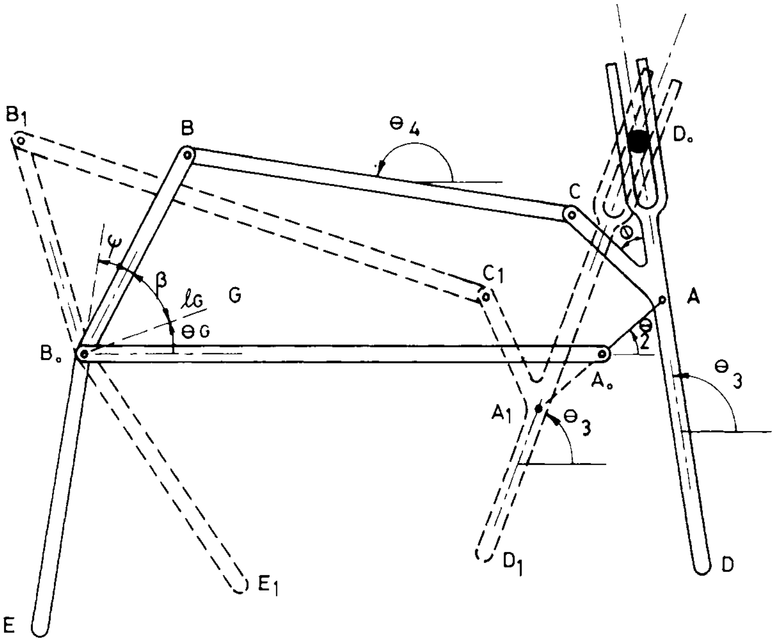

FIG. 11. Duplicate $R$-3 on a platform (arm not shown).

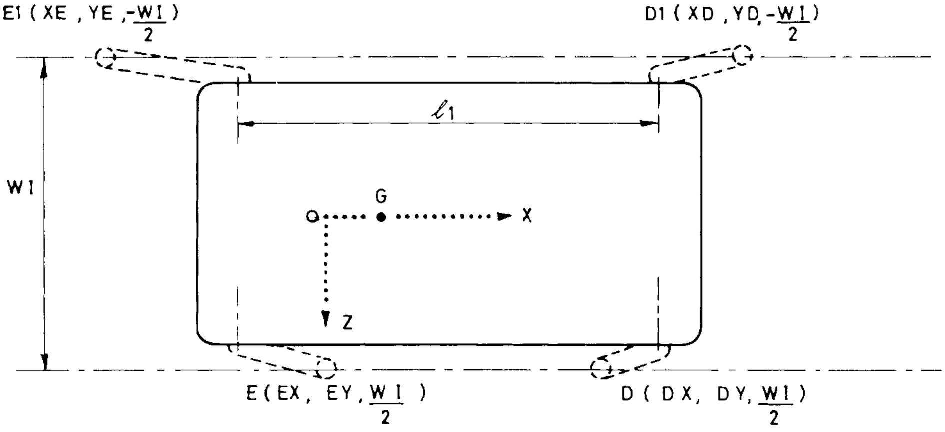

FIG. 12. Top view of the suspended robot (arm not shown).

Thus, the position vector for the center of mass in the suspended state (Fig. 11, 12, and Table 4).

$$R_G = EB_o\,[\cos(\beta + \psi)\, i + \sin(\beta + \psi)\, j] + l_G\,(\cos \Theta_G\, i + \sin \Theta_G\, j) \qquad (6)$$

can now be transformed by the use of Eqn 3 to express the position of $G$ in actual walking.

When feet $D$ and $E_1$ start tracing in the next half cycle, Eqn 4 and 5 take the form

$$\tan \Phi = [DY - EY] \,/\, [DX - EX] \qquad (7)$$

$$\tan \psi = [EY - YE] \,/\, WI \qquad (8)$$

The position vector for the center of mass is then (Fig. 11)

$$R_G = EB_o\,[\cos(c + \psi)\, i + \sin(c + \psi)\, j] + EEi + l_G\,(\cos \Theta_G\, i + \sin \Theta_G\, j) \qquad (9)$$

where $EE$ is the displacement in the $X$ direction (Fig. 12) during the previous half cycle, and $c$ is the value of $\beta$ at a phase angle of 180°.

Figure 13 illustrates the variation in the $x$-$y$ displacement of $G$ during a complete cycle for the set of dimensions given in Table 4. It is noted, in Fig. 13, that the center of mass moves a total of 22.5 cm in the $x$-direction, and there is a maximum vertical movement of 1.9 cm. The sideways ($z$-direction) movement per cycle is only 0.03 cm in either direction, as may be verified. Kinematics of the mainframe is presented elsewhere[5].

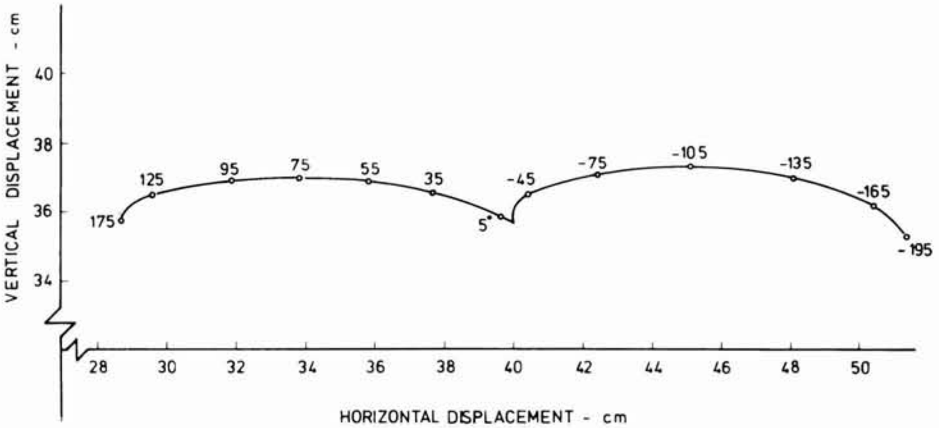

FIG 13. Displacement of the center of mass over one cycle.

## Concluding Remarks

Figure 14 shows the robot after assembly, complete with the arm but without its computer and electronics. The wheels on the rear feet were fitted with one-way

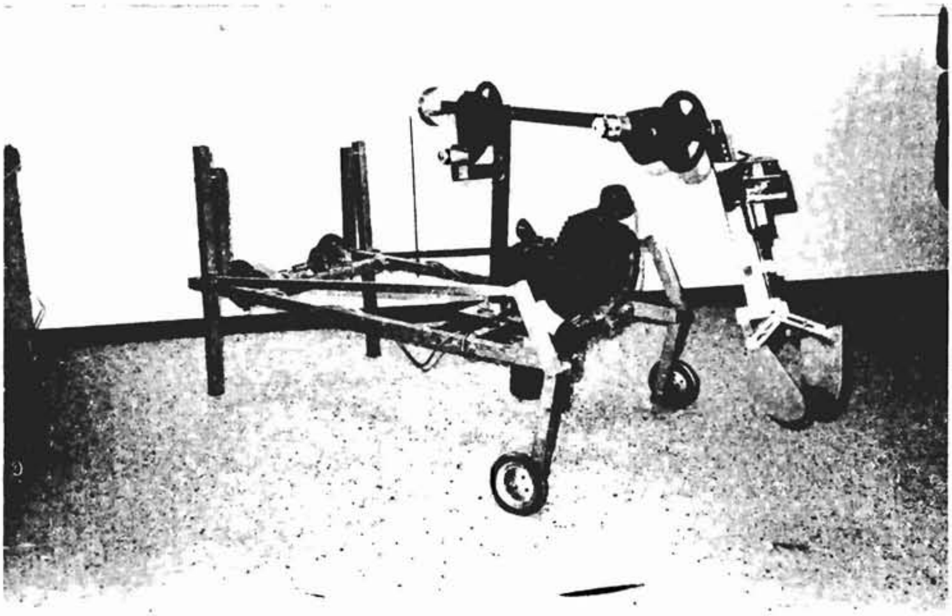

FIG. 14. The teaching and demonstration robot.

An analogous procedure yields a maximum rise of 6.3 cm for the front foot.

clutches to minimize drag when not tracting, and also to enhance the obstacle overriding ability.

Initial trials prior to computer controlled operation demonstrated smooth and stable walking, accompanied by a soft thumping sound each time a front foot touched the ground.

It is clear that the time is coming when robots will be employed on a wide scale in many industries. The need to train the technical manpower for the robotic age is apparent. It is anticipated that the introduction of this unique robot as well as other educational robots as part of the training programs will prove to be of much benefit.

## References

[1] **Raibert, M.H.** and **Sutherland, I.E.,** Machines that walk. *Scient. Am.* **248**(1): 44-53 (1983).

[2] **Tuttle, S.B.,** *Mechanisms for Engineering Design,* Wiley (1967).

[3] **Hall, A.S.,** *Kinematics and Linkage Design,* Prentice-Hall (1961).

[4] **Soylemez, E.,** *Mechanisms,* METU Press, Ankara (1979).

[5] **Mannaa, A.R., Dehlawi, F.** and **Akyurt, M.,** A stroking mechanism for special vehicle motion, *Int. J. Robotics Automation* (under publication).

[6] **Mannaa, A.R., Dehlawi, F.** and **Akyurt, M.,** Geometric design considerations for a three-link robot arm, *Computers in Industry* **7**(5): 395-400 (1986).

# دراسة متطلبات تصميم روبوت رباعي الأرجل

عبد الرؤوف محمد مناع ، فؤاد محمد أمين دهلوي* و مهمت مكرمين أكيورت
قسم هندسة الإنتاج وقسم الهندسة الكهربائية وهندسة الحاسبات ، كلية الهندسة*
جامعة الملك عبد العزيز ، جدة ، المملكة العربية السعودية

تمت ، في هذا العمل ، دراسة متطلبات تصميم روبوت « كائن آلي » رباعي الأرجل يستخدم لأغراض توضيحية تعليمية قادر على التقاط قطع خشبية تزن حوالي ٥٠٠ غرام ووضعها على منصة حمل على ظهره ثم نقلها إلى مناطق مختلفة لتفريقها هناك .

ولتحقيق ذلك تمت دراسة عدة تركيبات للتأكد من ملاءمة كل منها للحركة التي تعتمد على أربع أرجل . وقد اختيرت واحدة من هذه التركيبات لتصف حركة الروبوت أثناء المشي على أرض مستوية .

كما شمل العمل تصميم ذراع ثلاثية الوصلات مثبتة على الهيكل الرئيس للروبوت وتنتهي بمقبض لالتقاط الأشياء .